

Dear Reader.

This paper is an extended version of our SDM 2015 paper [a]. We are making this version available early as a service to the community (as Multi-Dimensional DTW has become ubiquitous with the prevalence of wearable sensors) and to solicit feedback and corrections.

[a] Mohammad Shokoohi-Yekta, Jun Wang and Eamonn Keogh (2015). On the Non-Trivial Generalization of Dynamic Time Warping to the Multi-Dimensional Case. SDM 2015.

Generalizing Dynamic Time Warping to the Multi-Dimensional Case Requires an Adaptive Approach

Mohammad Shokoohi-Yekta¹, Bing Hu², Hongxia Jin², Jun Wang³, Eamonn Keogh¹

¹ *University of California, Riverside*

² *Samsung Research America*

³ *University of Texas at Dallas*

¹{mshok002, eamonn}@cs.ucr.edu

²{bing.hu1, hongxia.jin}@samsung.com

³wangjun@utdallas.edu

Abstract— In recent years Dynamic Time Warping (DTW) has emerged as the distance measure of choice for virtually all time series data mining applications. For example, virtually all applications that process data from wearable devices use DTW as a core sub-routine. This is the result of significant progress in improving DTW’s efficiency, together with multiple empirical studies showing that DTW-based classifiers at least equal (and generally surpass) the accuracy of all their rivals across dozens of datasets. Thus far, most of the research has considered only the one-dimensional case, with practitioners generalizing to the multi-dimensional case in one of two ways, *dependent* or *independent* warping. In general, it appears the community believes either that the two ways are equivalent, or that the choice is irrelevant. In this work, we show that this is not the case. The two most commonly used multi-dimensional DTW methods can produce different classifications, and neither one dominates over the other. This seems to suggest that one should learn the best method for a particular application. However, we will show that this is not necessary; a simple, principled rule can be used on a case-by-case basis to predict which of the two methods we should trust at the time of classification. Our method allows us to ensure that classification results are at least as accurate as the better of the two rival methods, and, in many cases, our method is significantly more accurate. We demonstrate our ideas with the most extensive set of multi-dimensional time series classification experiments ever attempted.

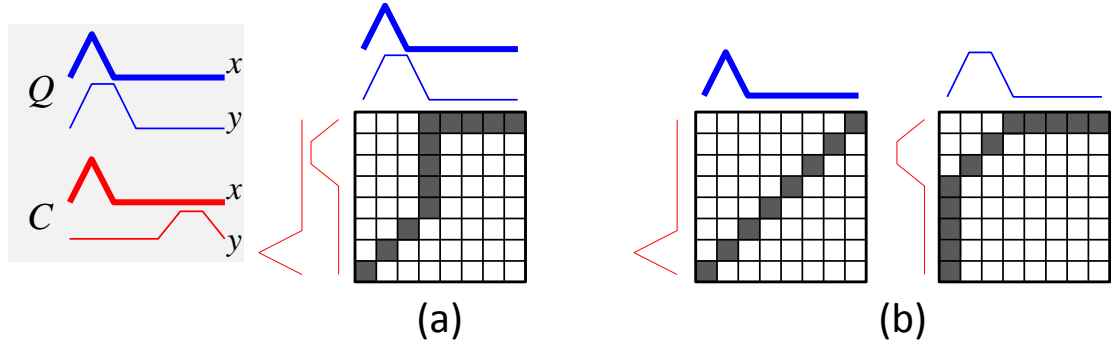
Keywords—*Dynamic Time Warping; Classification; Gesture Recognition; Wearable Devices*

1. Introduction

The research community seems to have converged on the belief that Dynamic Time Warping (DTW) is remarkably hard to beat as a time series distance measure, across a host of domain applications, and a host of tasks; including clustering, classification and similarity search [8][24]. Moreover, the most often cited reason for *not* using DTW, its relatively high time complexity, has recently become a non-issue. In particular, amortized over a subsequence search or subsequence monitoring task, DTW is slower than Euclidean Distance by less than a factor of two [29]. As a practical matter, carefully optimized DTW is *much* faster than all but the most carefully optimized implementations of Euclidean Distance [1]. For example, a modern cell phone, using the state-of-the-art DTW subsequence monitoring algorithm [29], can easily process streams arriving at several thousand Hertz. However, such devices only *produce* data at about 100Hz.

Virtually all attempts to improve time series classification in the last two decades have focused on the single-dimensional case, with the assumption that the generalization to the multi-dimensional case is trivial. There are two obvious ways DTW can be generalized to the multi-dimensional case: **Fig.1** gives a visual intuition, which we formalize later in this work. For clarity, we refer to the two methods as DTW_D and DTW_I (with D standing for Dependent and I for Independent).

The vast majority of researchers seem to think that it makes no difference which method is used, as evidenced by the fact that they usually do not explicitly bother to *tell* the reader.



$$(a) \text{DTW}_D(Q,C) = \text{DTW}(\{Q_x, Q_y\}, \{C_x, C_y\}) = 3.2$$

$$(b) \text{DTW}_I(Q,C) = \text{DTW}(Q_x, C_x) + \text{DTW}(Q_y, C_y) = 2.4$$

Fig.1 *top.left*) Two multi-dimensional time series. *a*) The DTW_D distance between them is 3.2. *b*) The DTW_I distance between them is 2.4. All elements of this visual key are formally defined below.

With some introspection we can see that there are actually several possibilities:

- There is no difference between DTW_D and DTW_I ; they produce the same values for all time series.

However, we can immediately dismiss this possibility; as shown in **Fig.1**, the two methods generally produce different distance values, and thus *could* produce different class labels if classifying an object using the Nearest Neighbor (NN) algorithm.

The next possibility seems to be the one *implicitly* assumed by the community:

- DTW_D and DTW_I *can* produce different distance values, but this makes no difference in the classification accuracy.

As we shall show, this is not the case. The choice of DTW_D vs. DTW_I *can* make a significant difference in the classification accuracy.

Given that DTW_D and DTW_I can have different classification accuracies, one might then imagine that the following is the case:

- While DTW_D and DTW_I can produce different classification accuracies, it so happens that one of the two is always superior on all problems. If we could prove, or experimentally demonstrate, this, we could “retire” the weaker measure.

This idea is tempting and has some precedents in similar situations in the literature. However, as we shall show, it is not the case. Datasets exist where DTW_D significantly outperforms DTW_I and vice-versa.

This would appear to be the end of the discussion. For a given problem, we can use cross-validation to determine which method to use, then simply hard-code it into our classifier. However, there are two reasons why this is *not* the last word. First, we do not have the luxury of cross-validation when we have very small training sets, a situation that is very common when *cold-starting* a gesture recognition system or when labeled data is expensive. Secondly, we are not done moving down the hierarchy of possibilities. In particular:

- For any given domain, it may be that, on an individual *class-by-class*, or even *exemplar-by-exemplar* basis, DTW_D and DTW_I can produce different results, and that we could predict which of the two methods to trust at classification time.

This possibility is less intuitive than the others. It is not clear that the utility of the measures should vary within a single domain, and, if it did, correctly predicting which measure was most likely to have been correct on a case-by-case basis seems like an untenable undertaking.

In this work, we show for the first time that this last possibility is correct. The utility of DTW_D and DTW_I varies on an instance-by-instance basis, and our technique, DTW_A ($DTW_{Adaptive}$), can predict at run time with high accuracy in terms of which of them is more likely to be correct [32].

Before leaving this section, we will give a visual and initiative example of our claims. While we normally think of DTW in the context of “true” time series, it has also been used to classify (suitably represented) text, spectrographs, shapes [18], and, as shown in **Fig.2**, *colors* [42].

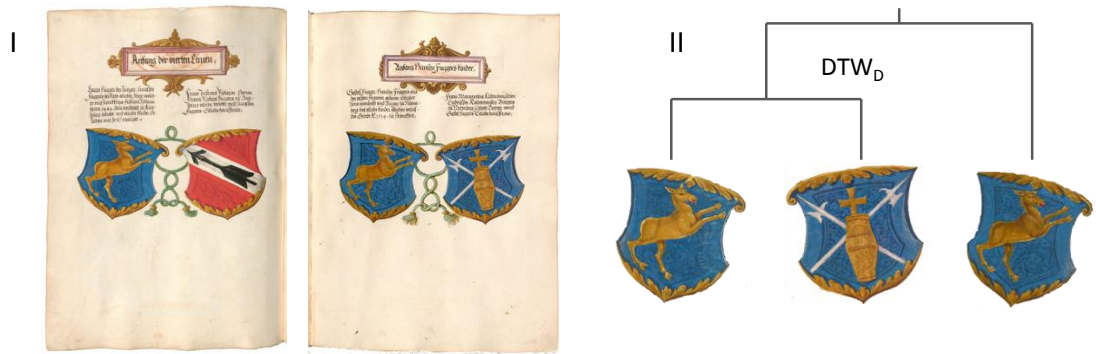


Fig.2 I) Two pages from a 16th century family history. The heraldic shield featuring the golden deer on a blue background is the family crest of Lucas Fugger. II) A clustering of three of the shields under DTW_D shows an unintuitive result, the two examples of the Fuggers are not grouped together.

Because color is typically represented in a three dimensional RGB space, it naturally forms a multidimensional time series, as shown in **Fig.3**.

The two pairs of examples shown in **Fig.3** are markedly different. In the pair of heraldic shields, each color needs to warp *independently*. A detailed, high-resolution examination of the images suggests why. While the blue background appears identical in each shield, the gold coloring of the deer is much darker in the uppermost example (this is easier to see in the large format images available at [43]). This difference is probably explained by the fact that the book took four years to produce, and maintaining exact hues over that time period would have been very difficult, especially with 16th century pigment technology.

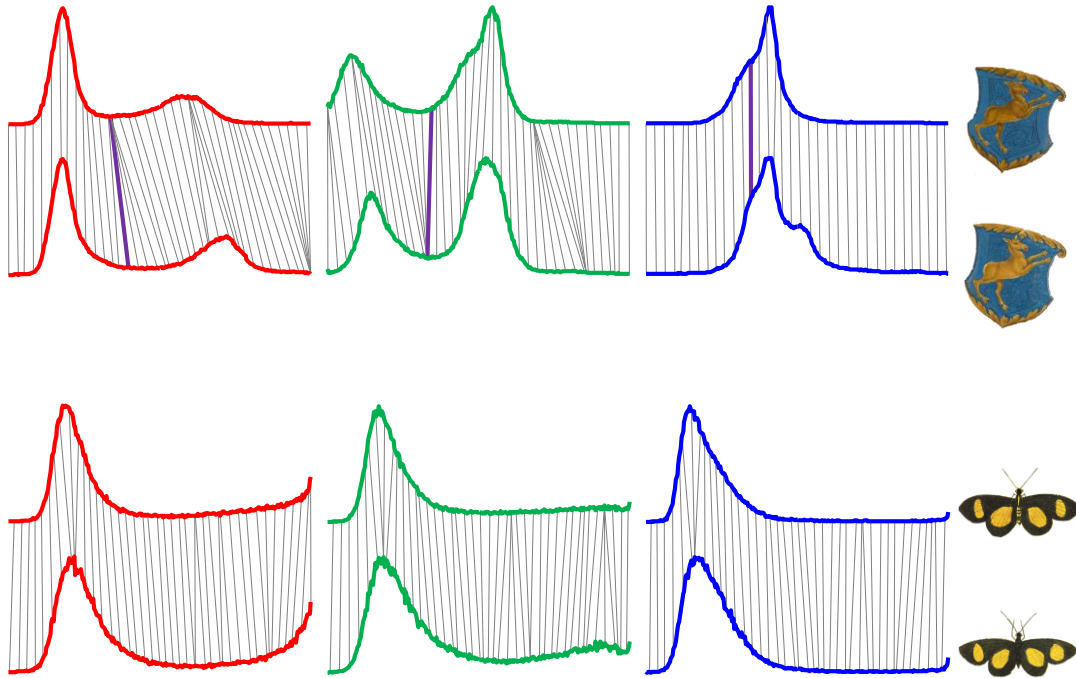


Fig.3 The color histograms of four objects taken from 16th century manuscripts. From left to right the red, green and blue channels are presented. Each channel has been *independently* aligned by DTW. *top*) The two examples from family crest of Lucas Fugger have radically different warpings in each of the three color channels, perhaps reflecting the fact that the book was created over a four year period. *bottom*) In contrast, the two butterfly examples have essentially identical alignments [3].

To make this clearer, we picked a single point just left of center on each channel of the lighter shield and recolored and thickened the hatch line that illustrates the warping. As we can see, in the blue channel the line is vertical, indicating no warping, in the green channel the line leans forward, and in the red channel the line leans backwards. This observation immediately explains the unintuitive clustering shown in **Fig.2.right**. By using DTW_D we forced all channels to warp in a single compromised way. If we simply use DTW_I we *do* obtain the correct clustering here.

This discussion seems to argue in favor of using DTW_I , at least for images. However, there are examples in which all color channels warp in the same way, as in the butterflies in **Fig.3.bottom** (see also Figure 5 of [42]). This happens if one image is simply sun-faded, or it can be an artifact of the scanning process. In such situations we are better off using DTW_D which finds the best warping by pooling evidence from all three sources of information.

Our work has two implications for the time series research community: we free researchers/implementers from having to decide which technique to use for their

problem; and, because $error(DTW_A)$ will be $minimum[error(DTW_D), error(DTW_I)]$, they can use our method safe in the knowledge that they did not choose the suboptimal method.

However, this greatly understates the case, as the correct inequality implied by our work is the more unintuitive $error(DTW_A) \leq minimum[error(DTW_D), error(DTW_I)]$. That is to say, on some datasets our method can be significantly more accurate than *either* of the rival methods.

2. Definitions and Background

We present the definitions of key terms that we use in this work. For our task at hand, each object in the dataset is a *time series*.

Definition 1: A *Time Series* $T = t_1, t_2, \dots, t_n$ is an ordered set of real values. The total number of real values is equal to the length of the time series. A dataset $\mathbf{D} = \{T_1, T_2, \dots, T_M\}$ is a collection of M such time series.

We are interested in multi-dimensional time series:

Definition 2: *Multi-Dimensional Time Series* (MDT) consist of M individual time series ($M \geq 2$) where each time series has n observations:

$$Q_1 = q_{1,1}, q_{2,1}, q_{3,1}, \dots, q_{n,1}$$

$$Q_2 = q_{1,2}, q_{2,2}, q_{3,2}, \dots, q_{n,2}$$

...

$$Q_M = q_{1,M}, q_{2,M}, q_{3,M}, \dots, q_{n,M}$$

If we wish to compare two time series, we could use the ubiquitous Euclidean distance. However, the DTW distance subsumes the Euclidean distance as a special case and has been shown to be significantly more accurate in virtually all domains [8][29]. Unlike the Euclidean distance's strict *one-to-one* alignment, DTW allows a *one-to-many* alignment, as illustrated in **Fig.1**. To align sequences using DTW, an n -by- n matrix is constructed with the (i^{th} , j^{th}) element being the squared Euclidean distance $d(q_i, c_j)$ between the points q_i and c_j . A warping path P is a contiguous set of matrix elements defining a mapping between Q and C . The t^{th} element of P is defined as $p_t = (i,j)_t$, so we have:

$$P = p_1, p_2, \dots, p_t, \dots, p_T \quad n \leq T \leq 2n - 1$$

The warping path that defines the alignment between the two time series is usually subject to several constraints: the warping path must start and finish in diagonally opposite corner cells of the matrix, the steps in the warping path are restricted to adjacent cells, and the points in the warping path must be monotonically spaced in time. In addition, virtually all practitioners using DTW also constrain the warping path in a global sense by limiting how far it may stay from the diagonal [8][24]. A typical constraint is the Sakoe-Chiba Band which states that the warping path cannot deviate more than R cells from the diagonal [8][24][29]. This constraint prevents pathological warpings (for example, a single heartbeat mapping to ten heartbeats) and is at the heart of the LB_{Keogh} lowerbounding technique, which is used in virtually all speedup techniques for DTW [1][8].

While there are exponentially many warping paths that satisfy the above conditions, we are only interested in the path that minimizes the warping cost:

$$(1) \quad DTW(Q, C) = \min \left\{ \sqrt{\sum_{t=1}^T p_t} \right\}$$

This path can be found using dynamic programming to evaluate the following recurrence, which defines the cumulative distance $D(i, j)$ as the distance $d(i, j)$ found in the current cell and the minimum of the cumulative distances of the adjacent elements [20][27]:

$$(2) \quad D(i, j) = d(q_i, c_j) + \min\{D(i-1, j-1), D(i-1, j), D(i, j-1)\} \text{ in which: } d(q_i, c_j) = (q_i - c_j)^2$$

While this recursive function is elegant and can be tersely implemented, in practice the community uses an *iterative* algorithm, which is faster and amiable to various early abandoning optimizations [1][8]. Moreover, the iterative algorithm implementation only constructs and considers a single column of the matrix at a time and, thus, has a space complexity of just $O(n)$.

The Euclidean distance between two sequences is a special case of DTW, where the t^{th} element of P is constrained such that $p_t = (i, j)_t$, $i = j = t$. This review of DTW is necessarily brief; we refer the interested reader to [1][8][20][27] for more details.

2.1 Generalizing to the Multi-Dimensional Case

The DTW distance, as formalized in Eq. 2, is applicable to only single-dimensional time series, leaving open the question of how to extend it to the multi-dimensional time series (MDT) case. Consider both Q and C as two M -dimensional time series; we show two possible approaches for doing this, DTW_I and DTW_D :

Definition 3: DTW_I is the cumulative distances of all dimensions independently measured under DTW. If $DTW(Q_m, C_m)$ is defined as the DTW distance of the m^{th} dimension of Q and the m^{th} dimension of C , we can write DTW_I as:

$$(3) \quad DTW_I(Q, C) = \sum_{m=1}^M DTW(Q_m, C_m)$$

In Eq. 3, each dimension is considered to be independent, and DTW is allowed the freedom to warp each dimension independently of the others. The case when M is two was shown in **Fig.1.b**.

We can also compute the multi-dimensional DTW in a manner that forces all dimensions to warp identically, in a single warping matrix. In other words, the independence of dimensions is no longer allowed, and we assume mutual dependence between all dimensions. We define DTW_D as:

Definition 4: DTW_D is calculated in a similar way to DTW for single-dimensional time series (Eq. 2), except that we redefine $d(q_i, c_j)$ as the cumulative squared Euclidean distances of M data points instead of the *single* data point used in the more familiar one-dimensional case. Formally, if $q_{i,m}$ is the i^{th} data point in the m^{th} dimension of Q and $c_{j,m}$ is the j^{th} data point in the m^{th} dimension of C , we replace $d(q_i, c_j)$ in (Eq. 2) with:

$$(4) \quad d(q_i, c_j) = \sum_{m=1}^M (q_{i,m} - c_{j,m})^2$$

To make our distance measure invariant to scale and offset, we need to *z-normalize* each dimension of the time series before computing their DTW distance. As demonstrated in [17], even tiny differences in scale and offset rapidly swamp any similarity in shape. Note that this allows us to meaningfully compute either variant of the multi-dimensional DTW, even if the individual dimensions are not commensurate or are in different units, such as *accelerations* and *rotations*.

Using both DTW_D and DTW_I distance measures to classify a time series exemplar, T , four different cases may occur:

1. T gets correctly classified by both DTW_I and DTW_D .
2. T gets misclassified by both DTW_I and DTW_D .
3. T gets classified correctly by DTW_I but misclassified by DTW_D .
4. T gets classified correctly by DTW_D but misclassified by DTW_I .

We are only interested in cases 3 and 4. We call such exemplars *iSuccess* and *dSuccess*, respectively:

Definition 5: *iSuccess* is the set of time series exemplars that are classified correctly under DTW_I but misclassified under DTW_D .

Definition 6: *dSuccess* is the set of time series exemplars that are classified correctly under DTW_D but misclassified under DTW_I .

Having reviewed the necessary formal definitions, we are now in a position to introduce our observations about the relative merits of DTW_D and DTW_I .

3. Observations

We begin with some informal notation. We say a dataset is “in D ” if we expect DTW_D to achieve higher accuracy and “in I ” if we anticipate DTW_I will be more accurate. In the introduction we claimed that there are datasets in which we expect DTW_D to outperform DTW_I and vice versa. A natural question to ask is under what conditions we can expect each of these methods to be superior. As we shall see, one of the fundamental contributions of this work is to make this question moot by producing an algorithm that is always *at least as good* as the better choice. Nevertheless, it is instructive to ask and attempt to answer this question.

Assume that the data in question corresponds to an *event*. An event could be an arrhythmic heartbeat, the writing of the letter ‘z,’ a golf swing, a bird call, a self-driving car parallel parking, etc. Further assume that we have multi-dimensional time series recordings of such events. It is possible that each dimension is simply recording two views of the same physical phenomena. For example, consider the MFCC coefficients of the bird call shown in **Fig.4**.

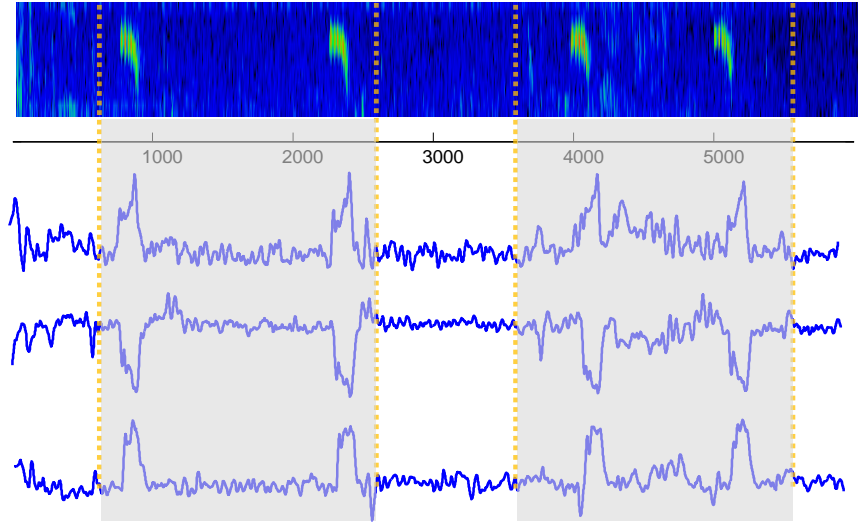


Fig.4 Three coefficients from the MFCC space of a Southern Chestnut-Tailed Antbird (*Myrmeciza hemimelaena*). This bird’s call is typically transcribed as “*klee-klee*” [11]; thus, the above shows two calls, the second being significantly briefer.

It is clear that while the coefficients are (somewhat) independent in the Y-axis values they can take on, they are *not* independent in the time axis. In the second bird call all the relevant peaks and valleys move by *exactly* the same amount in the time axis. Because of this structure, we strongly expect that this dataset is in *D*. In contrast, consider the *event* shown in **Fig.5** of a cricket umpire signaling TV-*Replay*, in which the umpire traces a rectangle representing a television screen.

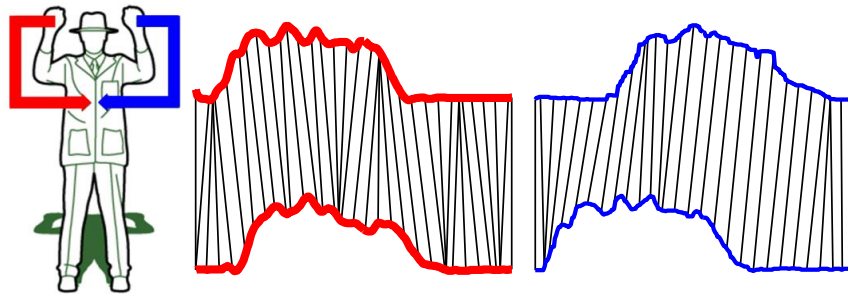


Fig.5 (left) A cricket umpire signaling “TV-*Replay*.” (right) The Dynamic Time Warping distance between two time series of the X-axis from the *right* and *left* hand.

Here we have measured a multi-d time series that consists of the X-axis acceleration of sensors worn on each wrist. Note that, in contrast to the bird call example, the two time series are very unlikely to be *perfectly* dependent in how they evolve in the time axis. Try as he might, the umpire could not move both hands in a *perfectly* symmetric fashion. There are at least two possible and non-exclusive sources of difference:

- **Lag:** Here, we imagine that the umpire favors his dominant hand, and the other hand follows at a more or less constant speed, but a fraction of a second behind.
- **Loose Coupling:** Here, the *event* does cause two or more things to happen, both of which are recorded as a time series, but there is more freedom in the performance of the event. For example, if the *event* is the umpire wishing to signal a `Leg-Bye`, he will tap his raised knee with this hand. However, while he typically uses his dominant hand to do this, he may touch *either* knee. Moreover, his “free” hand may rest by his side, or he may raise it, and even waive it slightly, to draw attention to the fact he is making a signal. This variability in performance means that two wrist-worn sensors are only very loosely coupled for this event.

In the next section, we will explicitly test the effects of these factors with some experiments. To do this we consider a dataset that we are sure is in D , and then we synthetically add increasing amounts of lag and loose coupling to see if this would move the dataset into I .

We consider a *handwriting* dataset, which we are confident is in D . Because we are considering the X and Y accelerations of the point of the writing tip of a pen, the two dimensions are *physically* coupled. Here, an *event* is the production of one of the twenty-six lower-case letters. We estimate the error rate of classification by randomly dividing the 5,000 objects into a stratified 1,000/4,000 train test split thirty times and reporting the average error rate.

It is critical to note that, in this dataset, if we were considering only the one-dimensional case, our synthetic modifications of the data would make essentially no difference to the distances DTW returns, or the overall error rate. As shown in **Fig.6**, even a huge change in the lag makes almost no difference to the single-dimensional DTW case.

Thus, all effects shown in the next two sections are due not to the effects of modifying the data objects per se, but to the effect this has on DTW_D and DTW_I .

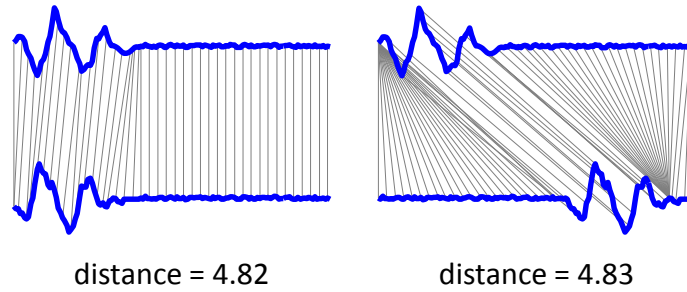


Fig.6 For the one-dimensional case, adding lag to one of the time series can change the *warping* drastically, without changing the *distance* by a significant amount.

3.1 The Effect of Lag

We induce lag in one of two ways. First, for each object we add *Random Lag* of K by shifting *just* the Y-axis by an amount randomly chosen from the range $[0, K]$. Second, we add a *Fixed Lag* variant by shifting *just* the Y-axis by increasing values of K . For clarity, in this variant all objects will have the same lag of exactly K . In **Fig.7** we show the effect of varying the amount of *Random Lag* from zero to forty.

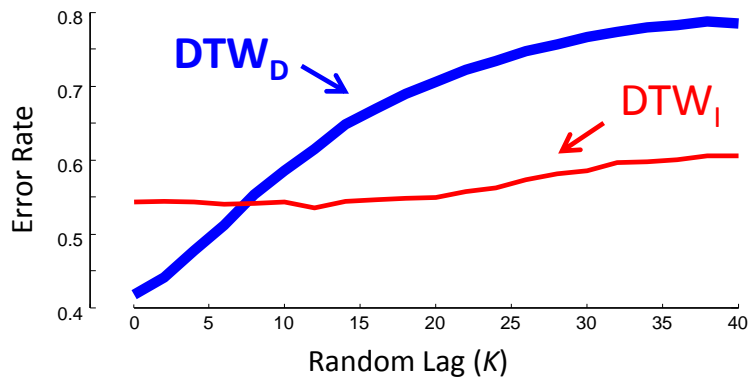


Fig.7 The effect of adding *Random Lag* on the classification accuracy of DTW_D and DTW_I .

In **Fig.8** we show the effect of varying the amount of *Fixed Lag*, again from zero to forty.

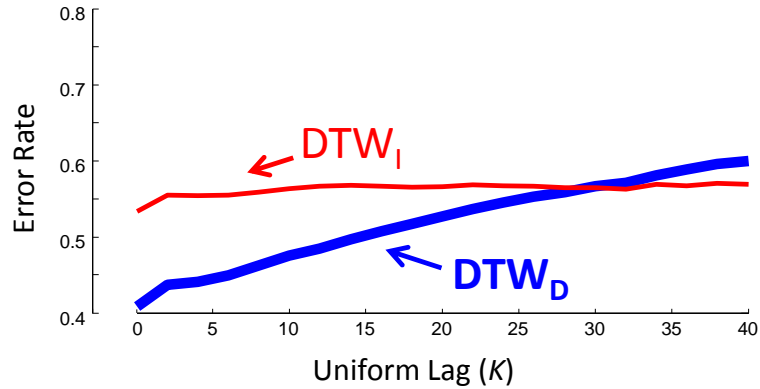


Fig.8 The effect of adding *Fixed Lag* on the classification accuracy of DTW_D and DTW_I .

If we consider just the values at either end of the range, this provides us with the first experimental evidence that datasets exist that are strongly in D , along with datasets (albeit *contrived* here) that are strongly in I . More generally, the trend lines in the figure confirm our claim that *Lag* is one of the elements responsible for datasets falling in D or I . Note that the effects are not small; the wrong choice of DTW_D or DTW_I here can almost double the error rate.

3.2 The Effect of Loose Coupling

We create synthetic loose coupling by adding increasing amounts of random warping to just the Y-axis of each exemplar. For brevity, and to enhance the flow of the presentation, we relegate the explanation (and the actual code) of how we do this to the supporting website [43]. However, we note that the modified data is plausible and realistic data. For example, if we use it to regenerate the original letters, they are readable and believable as a person's handwriting. **Fig.9** shows the effect of increasingly loose coupling.

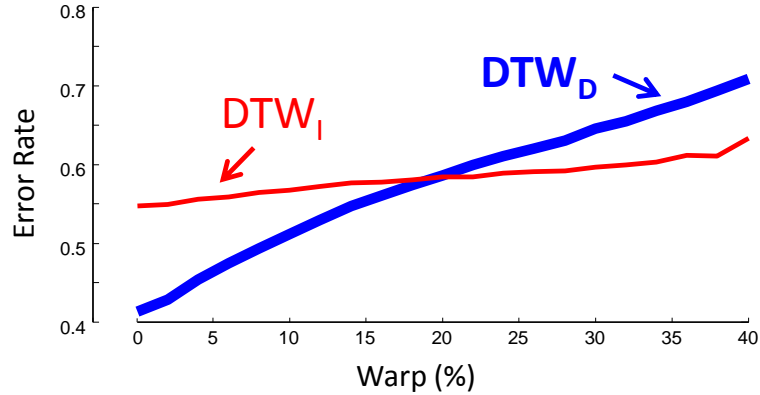


Fig.9 The effect of adding *Fixed Warping* on the classification accuracy of DTW_D and DTW_I .

Once again, these results provide us with evidence that some datasets are in D and some are in I , and that loose coupling can be a reason for this division.

3.3 Implication of Observations

At first blush we might interpret the above results as implying that all datasets lie on a spectrum between being strongly in D and strongly in I . If true, then the only task left to us is to discover where on the spectrum a dataset falls so that we can use the correct technique.

However, this idea has two difficulties. For some datasets we may not have enough training data to learn whether we are in D or in I with high confidence. The second issue is simply that the assumption that all *datasets* lie on such a spectrum misses a crucial point. It is possible that the suitability for DTW_D or DTW_I occurs at a *class-by-class* level, or even an *exemplar-by-exemplar* level, not at a *dataset-by-dataset* level.

It is easy to imagine such examples. Suppose we have accelerometers on both wrists of a tennis player, and our classification task is to label data into the following shot types {serve | forehand | lob | other}. For many exemplars we might expect DTW_I to work best, since the hands are generally loosely coupled in tennis. However, for some classes, such as the backhand, most players use a two-handed grip, temporarily coupling the two accelerometers. This would give us a *class-by-class*-level difference in the suitability of the warping technique. Moreover, some players, notably French professional Jo-Wilfried Tsonga, switch between one-handed

and two-handed back-hand shots during the game. This would give us an *exemplar-by-exemplar* level difference in the suitability of the warping technique.

3.4 Further Discussion

The reader may wonder why we need DTW_D at all. It appears that DTW_D is just a special case of DTW_I , and therefore unnecessary. In other words, if both warping paths created by DTW_I happen to be the same, the results are logically equivalent to DTW_D . Since there is nothing preventing this from happening, one might imagine that DTW_D is simply subsumed as a special case of DTW_I , and the results above are an error or anomaly of some kind.

The reason why we need both DTW_D and DTW_I is subtle and underappreciated. When we perform a DTW_I calculation and find it produces a relatively small distance, it *may* have achieved this with radically different warpings for each axis.

In contrast, DTW_D must use the same warping for *both* dimensions. Thus, in a sense, the fact that it could achieve a small distance, *in spite* of the same warping constraint, is *extra* evidence of similarity.

We can illustrate this with the simple experiment shown in **Fig.10**. Here we have three 2-dimensional time series. Subjectively we would surely group them $\{\{\mathbf{A},\mathbf{B}\},\mathbf{C}\}$, as \mathbf{B} is created by simply copying \mathbf{A} , shifting the “patterns” one place to the right, and adding a tiny “bump” in the 3rd value of \mathbf{B} . Nevertheless, if we cluster these objects with DTW_I , we get an extraordinarily unintuitive result, suggesting $\{\{\mathbf{A},\mathbf{C}\},\mathbf{B}\}$.

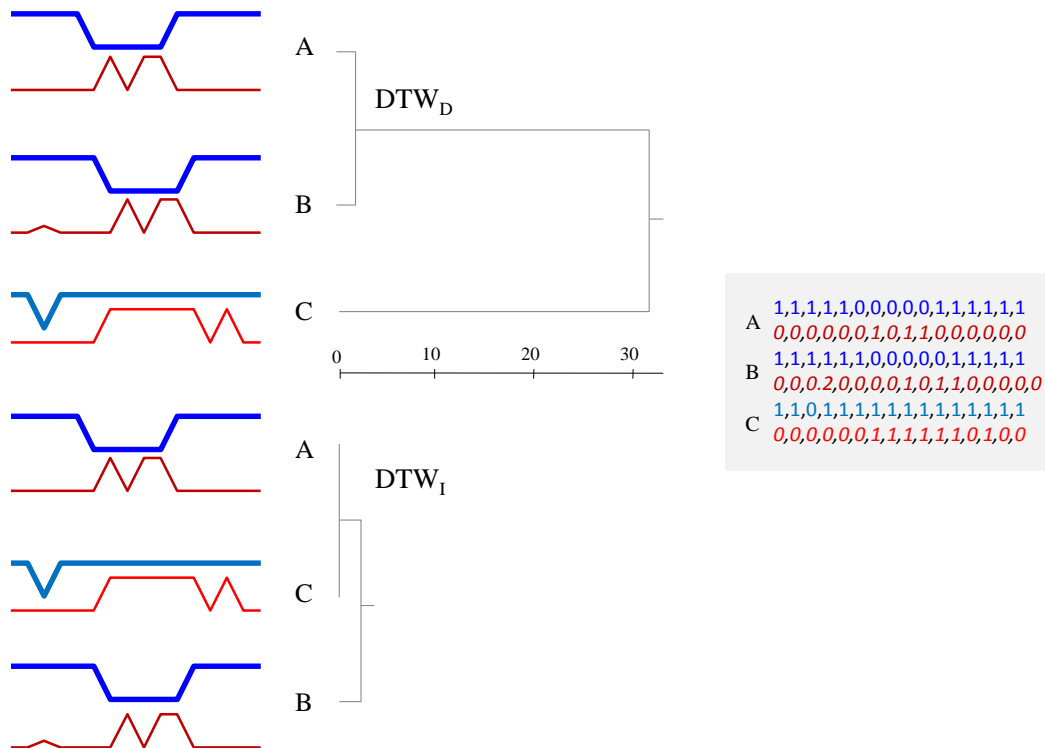


Fig.10 Three 2-dimensional time series (raw values shown in inset) single-linkage hierarchically clustered using DTW_D (top) and DTW_I (bottom). Here DTW_D produces an intuitive clustering, closely linking A and B, whereas DTW_I uses its greater representational flexibility to produce a bizarre result, finding A to be *identical* to C.

This may be easier to appreciate with an analogy. Imagine we have two distance measures, $NAME_D$ and $NAME_I$, that measure the distance between a target person’s name (say, “Anne Price”) and the set of names we find in a small address book. The underlying measure we assume is a string edit distance. The $NAME_I$ function calculates the most similar first and last names *independently*, perhaps finding “Anne Smith” and “Bob Price” in the address book to produce a distance of zero. In contrast, the $NAME_D$ function calculates the distances *dependently*, that is to say, from the *same* individual. Imagine that $NAME_I$ reports a distance of one, having found a person called ‘Anna Price’. While the latter distance of one is greater than the former distance of zero, we would almost certainly be more impressed by the similarity of the latter.

The example illustrated in **Fig.10** shows DTW_D outperforming DTW_I so forcefully that the reader may now wonder why we need DTW_I at all. As previously noted, DTW_D uses the same warping path for all dimensions to measure their distances. Therefore, DTW_D may not be a suitable distance measure for instances with lag,

simply because of using only one warping path (recall the three diverse warping paths for each of the color channels shown in **Fig.3.top**). For exemplars including lag between dimensions, DTW_I is capable of measuring the distances independently and being invariant to the lag. We illustrate this in **Fig.11**.

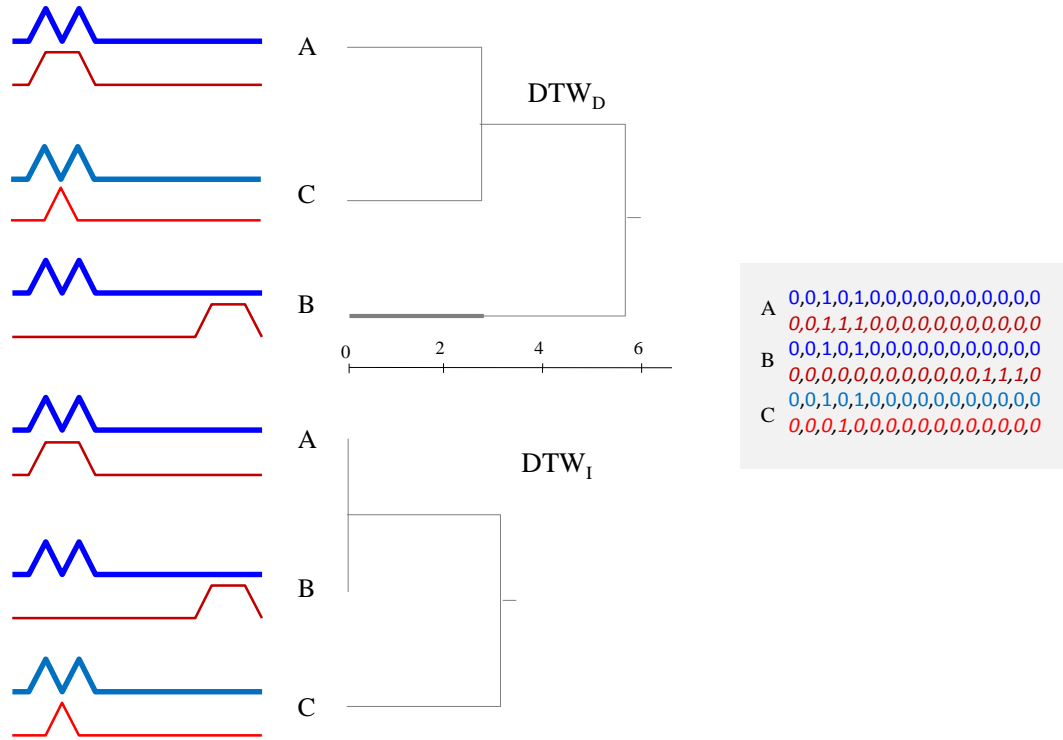


Fig.11 Three 2-dimensional time series (raw values shown in inset) single-linkage hierarchically clustered using DTW_D (top) and DTW_I (bottom). Here DTW_I produces an intuitive clustering, closely linking A and B, whereas DTW_D uses only one warping path to measure distances therefore producing a bizarre result, finding A to be *identical* to C. Compare to **Fig.10**.

Here instances **A** and **B** should belong to the same cluster since both are the same, except **B** includes a large lag in the second dimension (illustrated in red). As shown in **Fig.11**, DTW_D clusters **A** and **C** into the same subtree, simply because there is no lag in the second dimension of **C**. However, DTW_I correctly clusters **A** and **B** the same because the lag in the second dimension of **B** is ignored by DTW_I .

The reader may wonder if our observations are true but irrelevant, as we have only demonstrated our claims for contrived data up to this point. In our experimental section we give compelling evidence on several real-world datasets, but here we give a visually intuitive example. In **Fig.12** we show two dimensions of the telemetry from an oil refinery. In the first day shown, these two time series have near-perfect correlation, suggesting a very tight coupling. However, in the first half of the next day

a connecting valve is closed, and the two time series become almost completely uncoupled.

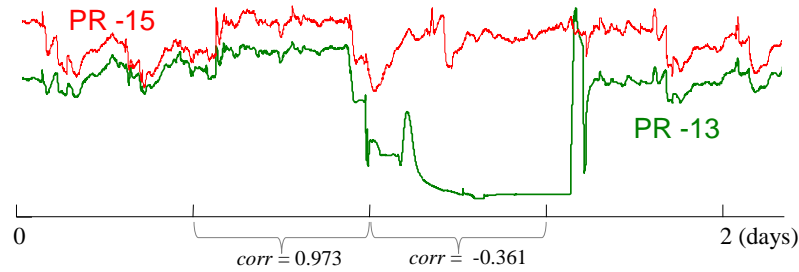


Fig.12 Two dimensions from a two-day sequence from the telemetry of a Delayed Coker. In the last twelve hours of Day One, the two pressure readings are tightly coupled, but in the first twelve hours of Day Two, they are almost completely uncoupled.

More generally, we have made similar observations in many datasets in scientific and medical domains. It seems quite common that the strength and type of *relationship* (*correlation* is not quite the right word here) between two time series can ebb and flow over time, and neither DTW_I nor DTW_{II} is always best.

Finally, before continuing, we must discount a solution that may have occurred to the reader, perhaps based on visual inspection of **Fig.1**. One might imagine that a large dissimilarity between the warping paths in DTW_I could indicate that the exemplar comparison in question is best suited to DTW_I . However, this is not the case. In general, it is possible that two warping paths could be arbitrarily different, but reflect *identical* DTW distances. In **Fig.13** we illustrate this with a toy example. While this example uses symmetric data to elucidate our point, this observation is more generally true.

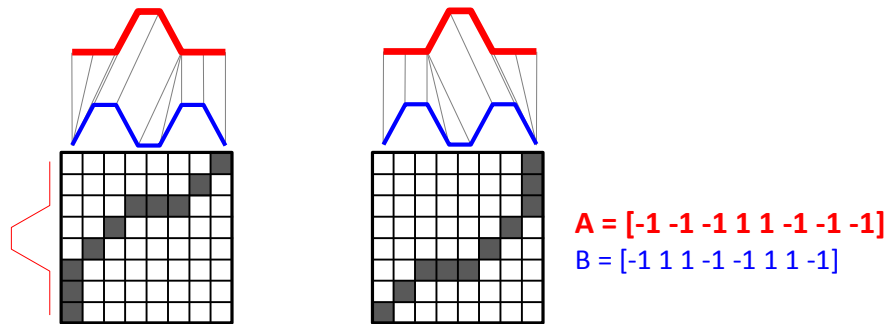


Fig.13 An example of two warping paths that are very different, but reflect *identical* DTW distances of 2.80.

4. Proposed Framework

In essence, our task reduces to a meta-classification problem. Given an instance to classify, we must first decide whether it is “an object best classified by DTW_I ” or “an object best classified by DTW_D .” More formally:

Problem Statement: Given that we are using NN-DTW to classify an exemplar Q , and that we have discovered the nearest neighbor to Q under both DTW_I and DTW_D , if the classes of the two nearest neighbors differ, predict the distance function most likely to be correct.

Our problem statement is superficially similar to a “gating network” in a Mixture of Experts (ME), a technique frequently used in neural networks and some other classifiers [40]. Using the divide and conquer principle, several “experts” that are either regression functions or classifiers are created such that they specialize in a particular region of the input space. The gating network defines those regions where the individual expert opinions are trustworthy, and uses a probabilistic model to combine the expert’s opinions.

There are many variants of ME (see [40] and references therein). However, in contrast to most versions, we have a much narrower task. We have exactly two experts, and we are “weighting” their opinions only in a strictly binary sense.

We propose the following solution to our problem. Offline, on the training data, we will compute a *threshold*. At query time, we will compute a score S , and choose which method to trust based on the value of S relative to the *threshold*. In order to best explain our framework, we first explain *how* our classification model works, given that a *threshold* has been learned from the *trainData*. Later, in Section 4.2, we consider the task of *learning* the *threshold*. If we have a lack of labeled data, we outline two possible approaches. We can either learn the *threshold* from a different dataset, from the same or similar domain, or we can simply hardcode the *threshold* to one, which gives us much of the benefit of our observation. We have explored both ideas in [43].

4.1 Adaptive Classifier for MDT

Table 1 outlines our classification algorithm. In line 1 the algorithm finds the nearest neighbor distance in the training set for Q under DTW_D , $minD$. In line 2 we find the nearest neighbor distance under DTW_I , $minI$. In line 3 the procedure divides $minD$ by $minI$, which is our scoring function, S . In lines 4 to 8 the algorithm compares our scoring function, S , to the previously learned *threshold*. If S is greater than the *threshold*, we believe that Q is most likely in I and thus return DTW_I as the distance measure for classification, whereas if S is less than or equal to the *threshold*, we predict that Q is most likely in D , and the function returns DTW_D .

Table 1 Adaptive classification algorithm

Procedure <i>adaptive_Classifier</i> (Q , <i>trainData</i> , <i>threshold</i>)	
Input: A time series query, Q , the labeled data, <i>trainData</i> , a <i>threshold</i> ;	
Output: An adaptive distance measure to classify Q , DTW_A ;	
1	$minD \leftarrow$ Nearest_Neighbor_Distance_D (Q , <i>trainData</i>);
2	$minI \leftarrow$ Nearest_Neighbor_Distance_I (Q , <i>trainData</i>);
3	$S \leftarrow minD / minI$;
4	if $S > threshold$
5	$DTW_A \leftarrow DTW_I$;
6	else
7	$DTW_A \leftarrow DTW_D$;
8	end if
9	Return DTW_A

We formally define our scoring function as:

$$(5) \quad S = \frac{\text{Nearest Neighbor Distance under } DTW_D}{\text{Nearest Neighbor Distance under } DTW_I + \epsilon}$$

The *epsilon* in the denominator is to prevent division by zero, a value that is theoretically possibility but never observed. While S can change in the range of $[\epsilon, \infty]$, in practice we find its value to always be in the range of $[0.5, 2]$.

Having explained our simple classification algorithm, all that remains is to explain how we set the threshold (and *why*). In fact, hardcoding the threshold to a value of exactly *one* works very well and allows the algorithm in Table 1 to beat the rival methods. However, we can further improve the accuracy by tuning the threshold, so in the next section we will explain how that is done.

4.2 Learning the Adjusted Threshold

In order to learn the *threshold* we use in Table 1, we first need to identify the *iSuccess* (def. 5) and *dSuccess* (def. 6) exemplars in the training set using cross validation (Table 3). As shown in Table 2, we consider four cases based on whether *iSuccess* and *dSuccess* are empty sets or not.

Table 2 Learning the adjusted threshold

Procedure <i>Learn_Threshold</i> (<i>trainData</i>)	
Input: Labeled data, <i>trainData</i> ;	
Output: Adjusted threshold, <i>threshold</i> ;	
1	$[S_{iSuccess}, S_{dSuccess}] \leftarrow \text{find_Scores}(\text{trainData});$
2	if ($S_{iSuccess} == \phi \ \&\& \ S_{dSuccess} == \phi$)
3	$threshold \leftarrow 1;$
4	else if ($S_{iSuccess} == \phi \ \&\& \ S_{dSuccess} \neq \phi$)
5	$threshold \leftarrow \max(S_{dSuccess});$
6	else if ($S_{iSuccess} \neq \phi \ \&\& \ S_{dSuccess} == \phi$)
7	$threshold \leftarrow \min(S_{iSuccess});$
8	else if ($S_{iSuccess} \neq \phi \ \&\& \ S_{dSuccess} \neq \phi$)
9	$threshold \leftarrow \text{Decision_Tree}(S_{iSuccess}, S_{dSuccess});$
10	end if

In line 1 we run the subroutine in Table 3 to find all the *S* scores for *iSuccess* and *dSuccess*, and then we consider four cases on the two sets. Line 2 is the case in which both sets are empty, so the problem (at least the training data) is independent of *D* or *I*, and picking either DTW_I or DTW_D will make no difference in classifying the data. Therefore, we assign the value one, an arbitrary number, to the *threshold* in line 3. We note that this case is possible, but we never observed it.

In line 4 we test to see if *S_{iSuccess}* is empty and *S_{dSuccess}* is non-empty. If so, the dataset is almost certainly in *D*, and we need to set the *threshold* such that the *S* score for all *dSuccess* exemplars will be less than the *threshold*. Therefore, in line 5 the *threshold* gets assigned to the maximum value of *S_{dSuccess}*.

The opposite case, in which *S_{dSuccess}* is empty and *S_{iSuccess}* is non-empty (line 6), offers evidence that the dataset is in *I*, and we need to set the *threshold* such that the *S* score for all *iSuccess* exemplars will be greater than the *threshold*. We ensure this (in line 7) by assigning the *threshold* to the minimum value of *S_{iSuccess}*.

In practice, the three cases above are rare, and in lines 8 to 10 we find the *threshold* for the most common case in which both $S_{iSuccess}$ and $S_{dSuccess}$ are non-empty sets. The best *threshold* is a value that maximizes the total number of $S_{iSuccess}$ with values greater than the *threshold* and $S_{dSuccess}$ with values less than the *threshold*. Finding such a *threshold* is essentially the decision tree problem of maximizing the *information gain* by finding the optimal split point. For more details on information gain, we refer the interested reader to [39][26].

Recall the function $find_Scores(trainData)$ called in Table 2. The function uses cross validation to find the two sets, $iSuccess$ and $dSuccess$, then calculates the S scores (Eq. 5) for all their exemplars. The algorithm is described in Table 3. In line 1 we apply cross validation to the entire $trainData$. In line 2 we calculate the nearest neighbor distance under DTW_D for each exemplar, and in line 3 we do the same under DTW_I . In lines 4 to 7, if the exemplar in the $trainData$ is classified correctly under DTW_D and misclassified under DTW_I , the S score (Eq. 5) is calculated and gets added to $S_{dSuccess}$. In line 8 to 11, if the exemplar is misclassified under DTW_D and classified correctly under DTW_I , we calculate the S score and add it to $S_{iSuccess}$.

Table 3 An algorithm to find $iSuccess$ and $dSuccess$ and compute S scores for all their exemplars

Procedure $find_Scores(trainData)$	
Input: Labeled data, $trainData$;	
Output: S scores for $iSuccess$ and $dSuccess$, $S_{iSuccess}$ and $S_{dSuccess}$;	
1	for $n \leftarrow 1$ to $size(trainData)$
2	$minD \leftarrow Nearest_Neighbor_Distance_D(trainData(n), trainData)$;
3	$minI \leftarrow Nearest_Neighbor_Distance_I(trainData(n), trainData)$;
4	if ($trainData(n).label == Nearest_Neighbor_D().label \ \&\&$
5	$trainData(n).label != Nearest_Neighbor_I().label$)
6	$S_{dSuccess}.add(minD / minI)$;
7	end if
8	if ($trainData(n).label != Nearest_Neighbor_D().label \ \&\&$
9	$trainData(n).label == Nearest_Neighbor_I().label$)
10	$S_{iSuccess}.add(minD / minI)$;
11	end if
12	end for

4.3 The Intuition Behind Our Scoring Function, S

In this section we explain the intuition behind our scoring function (Eq. 5), introduced in Section 4.1. We will show how the ratio of the nearest neighbor distance under DTW_D ($minD$) and DTW_I ($minI$) is capable of discriminating multi-dimensional time

series in I from exemplars in D . For any time series in I , each dimension is at least somewhat independent; therefore, exemplars that are from the same class and are warped/shifted independently in each dimension exist in the training set. **Fig.14.top** shows a time series in I , Q_I and its nearest neighbor in the training set, C_I .

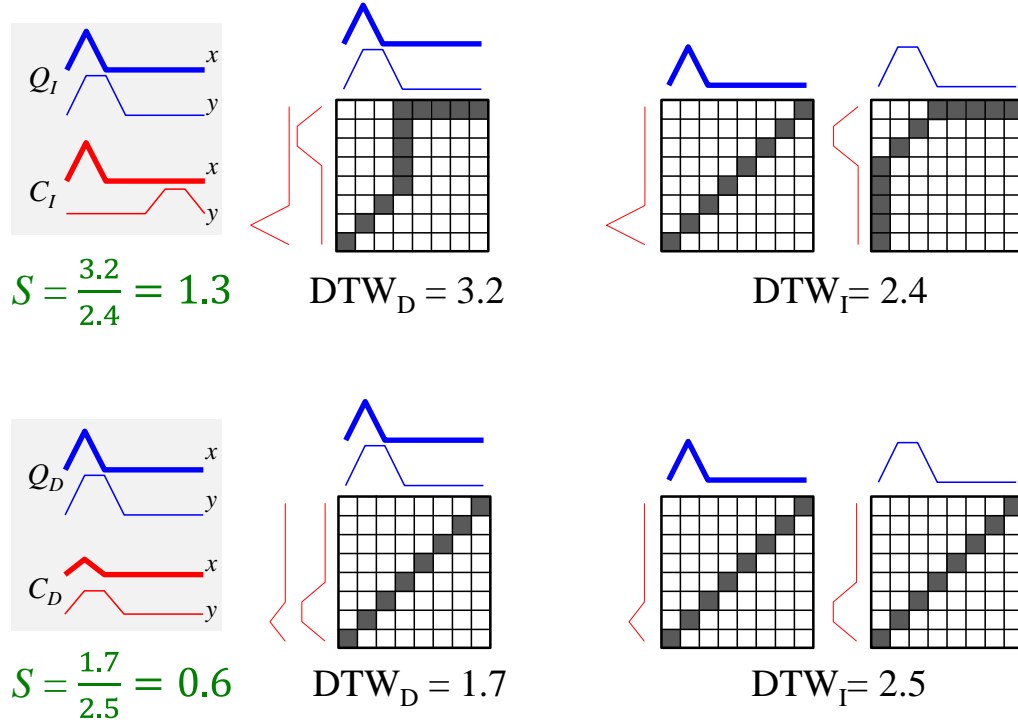


Fig.14 *top*) Computing the S score for a two-dimensional time series in I . *bottom*) S score calculation of a two-dimensional time series in D .

Note that in our proposed algorithm in Section 4.1 the nearest neighbors under DTW_I and DTW_D are not necessarily the same; however, for simplicity of presentation we consider C_I as the nearest neighbor under both DTW_I and DTW_D . Since Q_I is in I and its dimensions are warped independently, the DTW_I distance will be less than or equal to the DTW_D simply because DTW_I is allowed the freedom to find the nearest distance independently in each dimension. In **Fig.14.top**, DTW_I calculates the distance in two different paths, whereas DTW_D has only one path to pick which is a combination of the two paths in DTW_I and eventually produces a larger distance. For any instance in I , $minD$ is larger and $minI$ gets smaller; therefore, $minD/minI$ tends to be larger.

In **Fig.14.bottom** we show an instance, Q_D , which is in D . In this case the nearest neighbor in the training set, C_D , will be an exemplar in which both dimensions are

dependently warped. In such a case, the warping path for both dimensions in DTW_I are the same as, and similar to, the path in DTW_D . In contrast to the previous case, DTW_I does not take advantage of different warping paths in order to achieve a lower distance score compared to DTW_D . However, we show for the same warping path, the distance under DTW_I is larger than the DTW_D distance. Since DTW_D and DTW_I both take the same path, we can compare their cumulative distances in a meaningful way. If $q_{i,m}$ is the i^{th} data point in the m^{th} dimension of Q_D and $c_{j,m}$ is the j^{th} data point in the m^{th} dimension of C_D , for the two-dimensional case in **Fig.14.bottom**, we can show the following:

$$DTW_D(Q_D, C_D) = \sqrt{\sum_{i,j=1}^n [(q_{i,1} - c_{j,1})^2 + (q_{i,2} - c_{j,2})^2]} \prec$$

$$\sqrt{\sum_{i,j=1}^n (q_{i,1} - c_{j,1})^2} + \sqrt{\sum_{i,j=1}^n (q_{i,2} - c_{j,2})^2} = DTW_I(Q_D, C_D)$$

Accordingly, for a time series in D , $minD$ is smaller and $minI$ gets larger; therefore, $minD/minI$ tends to be smaller. We considered a two-dimensional time series here and assumed that for a query in I , the path in DTW_I and DTW_D are exactly the same; however, we can simply generalize the above illustration to dimensions greater than two, and for queries in I , different but similar paths for both DTW_I and DTW_D .

We have shown that our scoring function, S (cf. Eq. 5), tends to produce larger values for queries in I and smaller values for queries in D , as illustrated above; thus, our scoring function is capable of discriminating time series in I from exemplars in D . We will demonstrate the effectiveness of our scoring function with extensive experiments in the next section.

5. Experiments

We have designed all our experiments to ensure that they are *very* easy to reproduce. A supporting webpage [43] contains *all* the code, datasets, and raw data spreadsheets used in this work. Moreover, although this work is completely self-contained, the webpage contains additional experiments for the interested reader.

In addition to comparing to DTW_D and DTW_I , we also compare to the classification using each *individual* dimension, which we refer to using the notation $DTW_{(1st)}$, $DTW_{(2nd)}$, etc.

It is important to note that all experiments use *exactly* the same base algorithm, one nearest neighbor, and *exactly* the same train/test splits. Thus, any differences in results can be attributed solely to the distance measure used.

It is known that the warping window width can slightly affect the classification accuracy. As this issue is orthogonal to our work, we simply set the warping window constraint for DTW to be 20% for all experiments [8].

5.1 Recognition of Cricket Umpire Signals

Cricket is a very popular game in British Commonwealth countries. The game requires an umpire to signal different events in the game to a distant scorer/bookkeeper. The signals are communicated with motions of the hands. For example, `No-Ball` is signaled by touching each shoulder with the opposite hand, and `TV-Replay`, a request for an off-field review of the video of a play, is signaled by miming the outline of a TV screen (*cf.* **Fig.5**). A complete dictionary of signals can be found in [43].

The dataset introduced in [19] consists of four umpires performing twelve signals, each with ten repetitions. The data, recorded at a frequency of 184Hz, was collected by placing accelerometers on the wrists of the umpires. Each accelerometer has three synchronous measures for three axes (X , Y and Z). Thus, we have a six-dimensional MDT from the two accelerometers and we can combine any number of them to create a multi-dimensional classification problem. **Fig.15** shows the data for two example signals, `Six` and `Leg-Bye`. To signal `Six`, the umpire raises both hands above his head. `Leg-Bye` is signaled with a hand touching the umpire's raised knee three times.

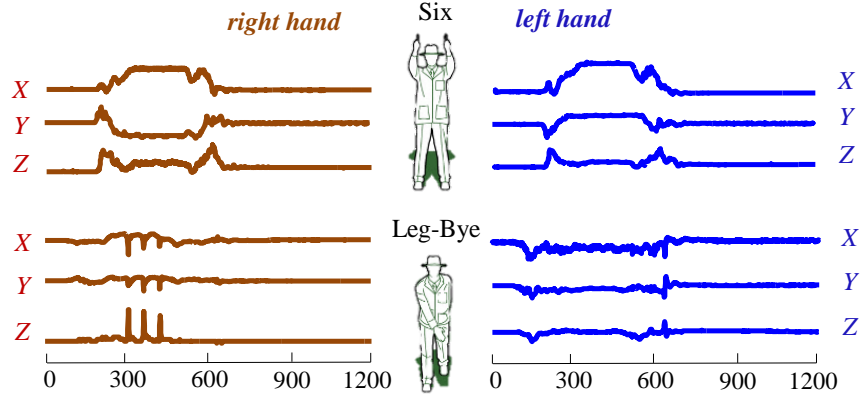


Fig.15 X , Y and Z acceleration data from the *right hand* (left), a representation of the umpire's body position (center), and the X , Y and Z acceleration data from the *left hand*, for the two umpire signals Six and Leg-Bye.

We used 40% of the data for training and use the rest as testing data. The classification results using various combinations of dimensions are shown in Table 4.

Table 4 Classification error rates on the cricket data

Data	$DTW_{(1st)}$	$DTW_{(2nd)}$	DTW_I	DTW_D	DTW_A
$X_{right_X_{left}}$	0.26	0.27	0.13	0.20	0.11
$Y_{right_X_{left}}$	0.17	0.27	0.07	0.04	0.03
$X_{right_Y_{left}}$	0.26	0.14	0.07	0.10	0.06
$Y_{right_Y_{left}}$	0.17	0.14	0.04	0.03	0.03
$Z_{right_Z_{left}}$	0.18	0.18	0.07	0.06	0.04
$Z_{right_X_{left}}$	0.18	0.27	0.07	0.04	0.04

Note that *all* combinations support our original claims that neither DTW_D nor DTW_I dominates the other, and that on all datasets, DTW_A is *at least as* accurate as the better of DTW_D and DTW_I , and often *more* accurate.

Above we considered only *pairs* of dimensions, however, the results generalize for any-sized subsets of dimensions. Obviously, adding more dimensions does not guarantee improved accuracy. In [13] the authors outline a strategy for choosing *which* dimensions to add to an MDT. Note, however, that this issue is completely orthogonal to our contributions; Table 4 suggests that whatever set of dimensions you choose, you are better off with DTW_A than any other method.

5.2 Accelerometer-Based Gesture Recognition

There is increasing interest in using gesture commands for interacting with and controlling external devices. The results in [16] suggest that different people often have different interpretations of even simple gestures, and thus it is necessary to *learn* personalized classifiers on an individual basis.

A widely used benchmark dataset, introduced in [22], consists of the performances of the gestures shown in **Fig.16** by eight participants. To produce realistic variability in performance, the data was collected on multiple days over three weeks. On each day the participant held a Nintendo Wii remote and repeated each of the eight gestures ten times.

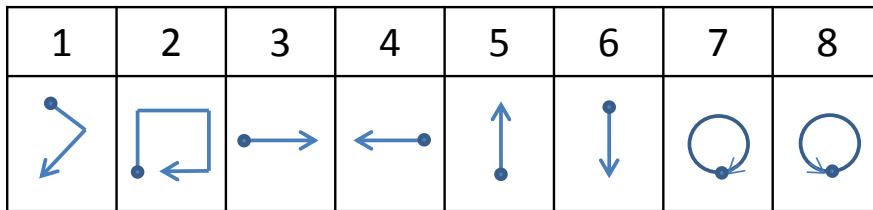


Fig.16 Gesture vocabulary adopted from [16]. The dot denotes *the start* and the arrow *the end* of the gesture.

The dataset consists of 4,480 gestures in total: 560 for each participant. The accelerometer has three axes (X , Y and Z); thus, we have a three-dimensional MDT form, and we can combine them to create a two or three multi-dimensional classification problem. We combined every pair of dimensions to create all possible two-dimensional time series and combined all three for the three-dimensional case. The classification results are shown in Table 5.

Table 5 Error rates for gesture recognition

Data	DTW _(1st)	DTW _(2nd)	DTW _(3rd)	DTW _I	DTW _D	DTW _A
X_Y	0.34	0.48	-	0.23	0.18	0.18
X_Z	0.34	0.41	-	0.13	0.13	0.12
Y_Z	0.48	0.41	-	0.26	0.24	0.23
X_Y_Z	0.34	0.48	0.41	0.11	0.09	0.08

As before, the results support our claim that DTW_A is *at least as* accurate as the better of DTW_D or DTW_I.

5.3 Word Recognition from Articulatory Movement Data

Silent “speech” recognition may potentially facilitate oral communication in people with severe voice impairments, for example, after laryngectomy, a surgical removal of larynx due to the treatment of cancer [36][37][38]. Silent speech recognition is to recognize words or sentences from non-audio data (e.g., tongue and lip movement data) [37]. An Electromagnetic Articulograph (EMA) [41] is an apparatus used to measure the movement of the tongue and lips during speech. The motion tracking using EMA is registered by attaching small sensors on the surface of the articulators (e.g., tongue and lips). The spatial accuracy of motion tracking using EMA AG500 is 0.5 mm [41]. We consider the EMA dataset in [36] which contains data collected from multiple native English native speakers producing 25 words. Twelve sensors were used in data collection, each providing X , Y and Z time-series positions with a sampling rate of 200 Hz. As shown in **Fig.17** the sensors are located on the forehead, tongue; from tip to back in the midline, lips and jaw. The three head sensors (Head Center, Head Right, and Head Left) attached on a pair of glasses were used to calculate head-independent movement of other sensors. Tongue sensors were named T1, T2, T3, and T4, from tip to back. For more details about the data collection procedure and description, please refer to [36].

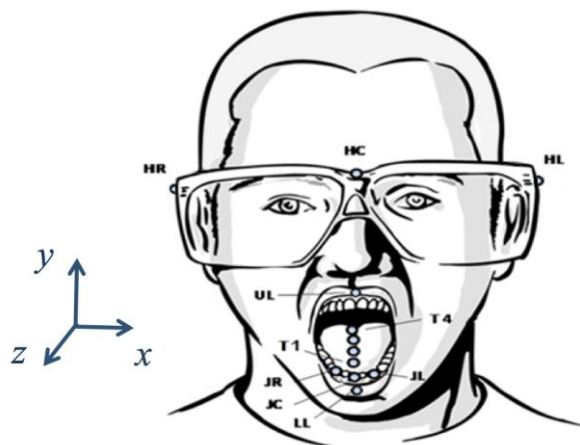


Fig.17 The coordinate system and sensor locations on a participant’s forehead, tongue, lips, and jaw in data collection using EMA. Labels are described in text.

Of the total of 36 available dimensions, for brevity and simplicity, we show only some random combinations of dimensions extracted from the sensors on the tongue

tip (TI), the upper lip (UL) and lower lip (LL). The classification results are shown in Table 6.

Table 6 Classification error rates on the continuous articulatory movement dataset

Data	DTW _(1st)	DTW _(2nd)	DTW _(3rd)	DTW _I	DTW _D	DTW _A
TI_Z-UL_X	0.34	0.59	-	0.25	0.31	0.25
TI_Y-UL_Y	0.38	0.55	-	0.22	0.15	0.13
TI_Z-LL_Z	0.34	0.47	-	0.17	0.10	0.10
TI_Z-LL_Y	0.34	0.48	-	0.20	0.12	0.11
TI_Y-LL_Y	0.38	0.48	-	0.21	0.14	0.14
TI_Y-TI_Z	0.38	0.34	-	0.24	0.15	0.15
$TI_X-TI_Y-TI_Z$	0.32	0.38	0.34	0.15	0.10	0.10
$TI_X-TI_Y-UL_Y$	0.32	0.38	0.55	0.16	0.18	0.14
$TI_Y-TI_Z-LL_X$	0.38	0.34	0.67	0.12	0.08	0.08
$TI_Z-LL_X-LL_Y$	0.34	0.67	0.48	0.14	0.12	0.10

Yet again, the results support our claim that DTW_A is *at least as accurate as the better* of DTW_D or DTW_I.

5.4 Revisiting the Semi-Synthetic Data

We reconsider the handwriting data set used in Section 3. Recall that the data is *real*, but manipulated in ways such that it changed from being in D to being in I . In **Fig.18** we revisit these problems, this time using DTW_A. Once again these experiments offer strong support for our claims about DTW_A dominating DTW_I and DTW_D.

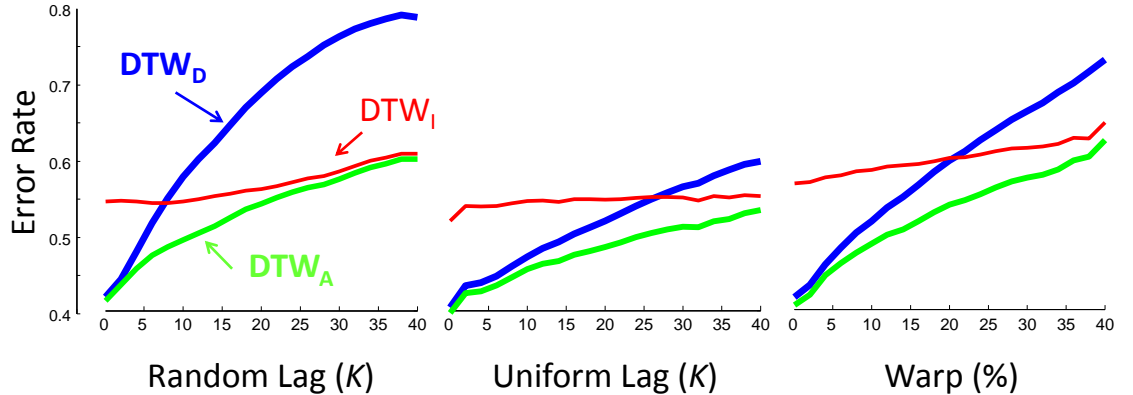


Fig.18 The experiments shown in **Fig.7**, **Fig.8** and **Fig.9**, revisited using the DTW_A technique.

5.5 Human Activity Recognition Using Smart Watches

Providing accurate and exploitable information on human activity has become an active field in pervasive computing [9][21][9]. Activity recognition using a smart watch has the potential to be highly useful in modern healthcare by monitoring the patients' activities and automatically reporting summaries to healthcare providers

[30]. In order to detect a specific set of gestures or behaviors during daily activities we can simply use a *rejection threshold*, which classifies the target gestures from (the much larger space of) non-target activities [14]. However, in order to detect such gestures/behaviors we need to know the best distance measure to classify the gestures. For this purpose we designed a simple experiment. We asked two users to wear a Samsung Gear 2 and execute 100 performances of eight different gestures. We collected the accelerometer data (X , Y and Z) with a sampling rate of 50 Hz. The eight gestures performed by users and a sample accelerometer data is shown in **Fig.19**.



Fig.19 *left*) Sample accelerometer data (X , Y and Z) of a gesture. *middle*) A Samsung Gear 2 used to collect activity data. *right*) the eight different gestures considered in our experiments.

We combined every pair of dimensions to create all possible two-dimensional time series and combined all three for the three-dimensional case. The classification results are shown in **Table 7**.

Table 7 Error rates for activity detection using a smart watch.

Data	DTW _(1st)	DTW _(2nd)	DTW _(3rd)	DTW _I	DTW _D	DTW _A
X_Y	0.43	0.46	-	0.25	0.17	0.15
X_Z	0.43	0.50	-	0.28	0.15	0.12
Y_Z	0.46	0.50	-	0.33	0.15	0.15
X_Y_Z	0.43	0.46	0.50	0.22	0.12	0.12

As with previous experiments, the results support our claim that DTW_A is *at least as* accurate as the better of DTW_D or DTW_I .

5.6 Learning the Threshold with Sparse Training Data

The reader may wonder if it is possible to learn the *threshold* if we have little labeled data to work with. For example, this is a common situation when beginning to use a new gesture-based system (the so-called “cold start” problem).

As noted in Section 4.1 in our paper, simply hardcoding the threshold to a value of one gives us much of the benefit of our observation. However, tuning the threshold **does** help, and we want to obtain the best possible accuracy.

Without claiming to have completely solved this problem, we outline one possible approach here. Our idea is that we can learn the *threshold* from a different dataset from the same or similar domain. In essence this is a simple form of *transfer learning*.

For example, if a company releases a smartwatch with gesture recognition capabilities, a good “universal” threshold could be learned and set at the factory. This would allow the system to work well “out-of-the-box,” and possibly be refined and personalized over time.

We have conducted an experiment to demonstrate this idea. For the *Gesture Recognition* dataset in Section 5.2 in our paper, we combined all three dimensions of X , Y and Z from the accelerometer and created two completely disjointed datasets, G_1 and G_2 . We learned the *threshold* from G_1 and used the same *threshold* to classify G_2 . The results are shown in **Table 8**.

Table 8 The first and second row correspond to results for classifying G_2 with the threshold learned from G_2 and G_1 , respectively

Data	DTW _(1st)	DTW _(2nd)	DTW _(3rd)	DTW _I	DTW _D	DTW _A
$X_Y_Z(1)$	0.30	0.45	0.37	0.08	0.06	0.05
$X_Y_Z(2)$	0.30	0.45	0.37	0.08	0.06	0.06

The results tentatively suggest that by adopting the threshold value from a different dataset in the same domain, we can achieve approximately the same accuracy we would have achieved by learning the threshold from a (large sample) of the native dataset.

5.7 What causes a time series to be in D or I ?

For all of the experiments considered above, the data sets included a mixture of exemplars in I and D . If this was not true, DTW_A could not have had a lower error-rate. However, an interesting question we have glossed over thus far is *what* causes an individual time series exemplar to be in D or I ? Is it an intrinsic property of the individual exemplar itself or a property of the exemplar in relation to a particular data set? We conducted a wide-ranging investigation of the exemplars' characteristics in various domains to see if any feature(s) stands out as a discriminator of time series in I vs. in D . We considered the correlation, complexity, Euclidean distance, Minimum Description Length, etc. of dimensions and did not find any useful discriminator.

We have designed a simple experiment which strongly suggests (at least for the data set considered) that the existence of exemplars in I or D strongly depends on the entire data set. A time series, which is in I , may later be in D if we use a different training set for classifying that item. In addition, just the size of the training set can have a significant impact on whether exemplars fall in I or D .

Once again we revisit the handwriting data set we used in Section 3. In all iterations we randomly sample ten exemplars from each of twenty-six classes as the test set (a total of 260 items). In the first iteration we randomly pick only a single instance for each class and define it as the train set. Then we classify the test set using DTW_D and DTW_I separately and also count the number of items in $iSuccess$ and $dSuccess$ (cf. definitions 5 and 6). In the second iteration we randomly pick two instances for each class as the train set and repeat the same steps. We continue the iterations until we reach seventeen exemplars per class. The results are shown in **Fig.20**.

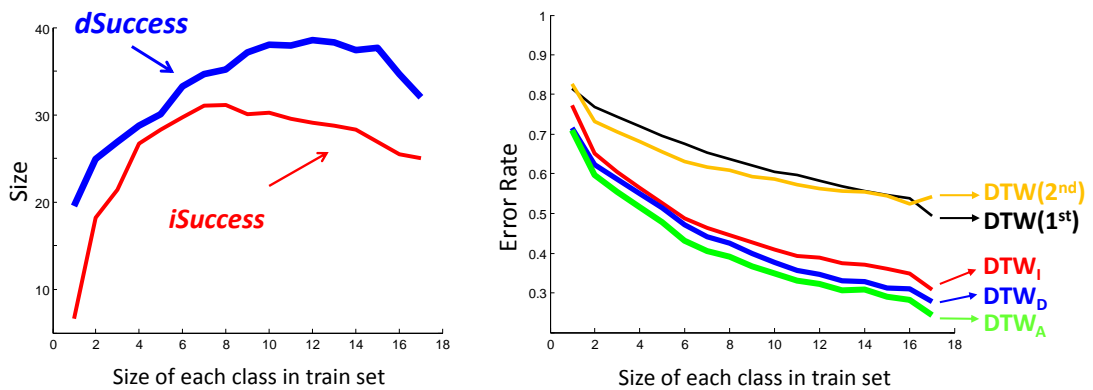


Fig.20 *left*) The number of elements in $iSuccess$ and $dSuccess$ for train sets of different sizes. *right*) The effect of data set size on accuracy of classification.

We believe we can interpret **Fig.20** as follows. First (and only incidentally here), **Fig.20.right** supports our claim that DTW_A is *at least as* accurate as *the better* of DTW_D or DTW_I , as the green curve for DTW_A dominates all the other approaches for the entire range of training data sizes. Note that all five approaches have almost the same (very high) error-rate when the training set is very small. This is simply because there is very little space for them to differ. In the limit, had we started one value to the left, with *zero* data, all approaches would have had the *exact* same error-rate, the default rate.

As the training dataset gets larger, all approaches benefit, just as we expect. However, DTW_A benefits the most. This is because as the training dataset gets larger, there is a greater possibility that some objects to be classified can benefit from choosing the more suitable of the two multi-dimensional variants of DTW. To see this more clearly, in **Fig.20.left** we measured the number of objects in *iSuccess* and *dSuccess* for the experiments shown in **Fig.20.right**. We see that for small train sets the number of items in *iSuccess* and *dSuccess* are low. However, when the size of the train set increases, the number of instances in *iSuccess* or *dSuccess* begins to increase in spite of the fact that the size of the test sets remains constant.

There is one observation in **Fig.20.left** that we have to explain. After some point, the number of items in *iSuccess* and *dSuccess* begins to *decrease*. Why is this? The reason is that, for large enough training sets, there is a greater chance that the nearest neighbor, under *both* DTW_I and DTW_D , will be the same (true) class. This will make our DTW_A unnecessary (but *not* harmful to accuracy). A similar effect has been shown for the error-rates of (one dimensional) DTW vs. ED classifiers (See **Fig.1** of [33]). For small datasets, DTW and ED often make different decisions about which item is the nearest neighbor, but as the datasets get larger they tend to agree more and more often, eventually converging to the same error-rate [33][28].

In a sense, these observations seem to cast limits on the utility of our proposed ideas. DTW_A will be no better (but critically, no *worse*) in the case that the training dataset is pathologically small or is arbitrarily large. However, the situation in between is clearly the most common. For example, in virtually all gesture recognition systems it is assumed that the user is willing to provide at least five to ten examples of a gesture so that we can estimate variability of performance [16][22][12][35][1][34]. But,

clearly, we do not expect an individual user to provide one thousand labeled examples of a gesture.

6. Related Work

We have deferred a discussion of related work until now when the reader can appreciate the nature of our contributions. While there are hundreds of research efforts that use DTW in a multi-dimensional setting [11][16][19][22][25][36], we are not aware of any work that discusses the relative merits of DTW_I and DTW_D , or even explicitly notes that they are alternatives. The vast majority of researchers seem to think that it makes no difference which method is used, as evidenced by the fact that they usually do not bother to explicitly *tell* the reader [22][1][1][15][34]. In paper [22] they define DTW as a dynamic programming algorithm, which calculates the matching cost and finds the corresponding shortest path. However, it is not clear how they generalize it to the multi-dimensional case. A handful of papers do mention that there exist two ways of computing dynamic time warping in multi-dimensional time series. For example, the authors in [25] choose DTW_D for classifying satellite images because they argue that satellite images have dependent dimensions in their time series. Other papers, such as [12][1][10], use DTW_D without pointing out the alternative approach of DTW_I . The authors in [35][6][23] use other methods similar to DTW_I such as adding up all dimensions and dealing with a single dimension time series. For instance, [6] applies DTW to the data obtained from the sum of all channels in different dimensions. The authors in [35] normalize and smooth each dimension and then use the total difference among dimensions to find the best synchronization with the regular DTW algorithm.

The ubiquity of multi-dimensional time series, especially given the recent explosion of interest in wearable devices, has produced significant research in speeding up DTW [29], choosing which subset of dimensions to use [13], choosing a setting for the warping window constraint [8], etc. However, all such work is orthogonal to (and compatible with) our contributions. We have created an annotated bibliography of which papers use DTW_I vs. DTW_D [43].

As we noted above, there is significant research in “gating networks” and related techniques for choosing which classifier to use on a given region of the input space

[40]. However, to the best of our knowledge, these ideas have never been applied to time series and are only superficially related to the task at hand.

7. Conclusions

In this work we demonstrate for the first time that of the two obvious ways to do multi-dimensional NN-DTW classification, neither is always superior. We show that the differences are not trivial, as the wrong choice can *double* the error rate. We introduce a simple algorithm that can pick the method that is most likely to predict the correct class on a case-by-case basis. Our algorithm is simple to implement, and its overhead is inconsequential in terms of both time and space.

For concreteness we have confined our remarks and empirical demonstrations to *classification* problems, but note that distance measures are at the heart of many time series data mining tasks, including clustering, summarization, motif discovery, and many forms of anomaly detection. In future work we will expand our consideration of our ideas to these tasks.

Finally, in this work we have focused on intuitively explaining our observations/ideas and showing strong empirical evidence for them. However, we plan to revisit our work with a more theoretical framework and prove several useful properties of DTW_A .

Acknowledgments

This research was supported by NSF IIS-1161997, NIH R01 DC013547, the Bill and Melinda Gates Foundation, the Vodafone's Wireless Innovation Project and a gift from Samsung.

References

- [1] J. Aach and G. M. Church. *Aligning gene expression time series with time warping algorithms*. *Bioinformatics* 17, no. 6 (2001): 495-508.
- [2] A. Akl, S. Valaee. *Accelerometer-Based Gesture Recognition via Dynamic-Time Warping, Affinity Propagation, & Compressive Sensing*. *Acoustics Speech and Signal Processing (ICASSP), 2010 IEEE International Conference on*, pp. 2270-2273. IEEE, 2010.
- [3] Seba, Albertus. *Locupletissimi rerum naturalium thesauri accurata descriptio, et iconibus artificiosissimis expressio, per universam physices historiam : Opus, cui, in hoc rerum genere, nullum par exstitit* (1734)
- [4] A. Al-Jawad, M. Reyes Adame, M. Romanovas, M. Hobert, W. Maetzler, M. Traechtler, K. Moeller and Y. Manoli, *Using multi-dimensional dynamic time warping for TUG Test instrumentation with inertial sensors*. 2012 IEEE Conference on, pp. 212-218. IEEE, 2012.

- [5] I. Assent, M. Wichterich, R. Krieger, H. Kremer, T. Seidl: *Anticipatory DTW for Efficient Similarity Search in Time Series Databases*. PVLDB 2(1): 826-837 (2009).
- [6] M. Bashir and J. Kempf. *Reduced Dynamic Time Warping for Handwriting Recognition Based on Multi-Dimensional Time Series of a Novel Pen Device*. International Journal of Intelligent Systems and Technologies, WASET 3, no. 4 (2008): 194.
- [7] Das Ehrenbuch der Fugger (The secret book of honour of the Fugger) -BSB Cgm 9460, Augsburg, ca. 1545 - 1548 mit Nachträgen aus späterer Zeit.
- [8] H. Ding, G. Trajcevski, P. Scheuermann, X. Wang, and E. J. Keogh. 2008. *Querying and mining of time series data: experimental comparison of representations and distance measures*. PVLDB 1, 2, 1542-52.
- [9] M. Ermes, J. Parkka, J. Mantyjarvi, and I. Korhonen. *Detection of daily activities and sports with wearable sensors in controlled and uncontrolled conditions*. Information Technology in Biomedicine, IEEE Transactions on 12, no. 1 (2008): 20-26.
- [10] R. Fernandes de Mello and I. Gondra, *Multi-Dimensional Dynamic Time Warping for Image Texture Similarity*. In Advances in Artificial Intelligence-SBIA 2008, pp. 23-32. Springer Berlin Heidelberg, 2008.
- [11] Field Guide to the Songbirds of South America The Passerines - Mildred Wyatt-Wold Series in Ornithology(2009) Robert S. Ridgely, Guy Tudor. University of Texas Press.
- [12] N. Gillian, R. Benjamin Knapp, S. O’Modhrain, *Recognition Of Multivariate Temporal Musical Gestures Using N-Dimensional Dynamic Time Warping*. NIME11 (2011).
- [13] B. Hu, Y. Chen, J. Zakaria, L. Ulanova, E. Keogh: *Classification of Multi-dimensional Streaming Time Series by Weighting Each Classifier’s Track Record*. ICDM 2013: 281-290
- [14] B. Hu, Y. Chen, and E. J. Keogh. *Time Series Classification under More Realistic Assumptions*. In SDM, pp. 578-586. 2013.
- [15] N. Kale, J. Lee, R. Lotfian and R. Jafari . *Impact of Sensor Misplacement on Dynamic Time Warping Based Human Activity Recognition using Wearable Computers*. Proceedings of the conference on Wireless Health, p. 7. ACM, 2012.
- [16] J. Kela, P. Korpipaa, J. Mantyjarvi, S. Kallio, G. Savino, L. Jozzo and D. Marca. *Accelerometer-based gesture control for a design environment*, Personal and Ubiquitous Computing, vol. 10, no. 5, pp. 285-299, 2006.
- [17] E. Keogh and S. Kasetty, *On the need for Time Series Data Mining Benchmarks: a survey and empirical demonstration*, Proc. ACM KDD 2002, pp. 102-111.
- [18] E. J. Keogh, L. Wei, X. Xi, S. H. Lee, M. Vlachos: *LB_Keogh Supports Exact Indexing of Shapes under Rotation Invariance with Arbitrary Representations and Distance Measures*. VLDB 2006: 882-893
- [19] M. H. Ko, G. West, S. Venkatesh and M. Kumar. *Online context recognition in multisensory system using dynamic time warping*. In Intelligent Sensors, Sensor Networks and Information Processing Conference, 2005.
- [20] J. B. Kruskall, and M. Liberman, *The symmetric time warping algorithm: From continous to discrete*. In *Time Warps, String Edits and Macromolecules*. Addison-Wesley, 1983.
- [21] O. D. Lara and M. A. Labrador. *A survey on human activity recognition using wearable sensors*. Communications Surveys & Tutorials, IEEE 15, no. 3 (2013): 1192-1209.
- [22] J. Liu, Z. Wang, L. Zhong, J. Wickramasuriya and V. Vasudevan, *uWave: Accelerometer-based personalized gesture recognition and its applications*, IEEE intl. Conf. Pervasive Computing and Communication (PerCom), 2009.
- [23] D. McGlynn and M. G. Madden. *An Ensemble Dynamic Time Warping Classifier with Application to Activity Recognition*. Research and Development in Intelligent Systems XXVII, pp. 339-352. Springer London, 2011.
- [24] P. Papapetrou, V. Athitsos, M. Potamias, G. Kollios, and D. Gunopulos. *Embedding-based subsequence matching in time-series databases*. ACM TODS 36, 3, 17, 2011.
- [25] F. Petitjean, J. Inglada and P. Gancarski. *Satellite Image Time Series Analysis under Time Warping*. IEEE Transactions on Geoscience and Remote Sensing, vol. 50-. 8, pp. 3081-95, 2012.
- [26] J. R. Quinlan, (1986). *Induction of Decision Trees*. Machine Learning 1: 81-106, Kluwer Academic Publishers.
- [27] L. Rabiner, and B. Juang, *Fundamentals of speech recognition*. Englewood Cliffs, N.J, Prentice Hall, 1993.
- [28] C. A. Ratanamahatana and E. Keogh. (2004). *Everything you know about Dynamic Time Warping is Wrong*. Third Workshop on Mining Temporal and Sequential Data, in conjunction with the Tenth ACM SIGKDD International Conference on Knowledge Discovery and Data Mining (KDD-2004), August 22-25, 2004 - Seattle, WA
- [29] T. Rakhthamanon, B. J. L. Campana, A. Mueen, G. E. A. P. A. Batista, M. B. Westover, Q. Zhu, J. Zakaria and E. J. Keogh: *Addressing Big Data Time Series: Mining Trillions of Time Series Subsequences Under Dynamic Time Warping*. TKDD 7(3): 10 (2013)

- [30] R. Rawassizadeh, B.A. Price., M. Petre. Wearables: *Has the age of Smartwatches finally arrived?*. in Communication of ACM, 2015. Vol 58, Issue 1
- [31] Y. Sakurai, C. Faloutsos, and M. Yamamuro. 2007. *Stream monitoring under the time warping distance*. ICDE, 1046-55.
- [32] M. Shokoohi-Yekta, J. Wang and E. Keogh. *On the Non-Trivial Generalization of Dynamic Time Warping to the Multi-Dimensional Case*. SDM 2015 (to appear).
- [33] J. Shieh, E. J. Keogh: *iSAX: disk-aware mining and indexing of massive time series datasets*. Data Min. Knowl. Discov. 19(1): 24-57 (2009)
- [34] J. Tang. *Extracting Commands From Gestures: Gesture Spotting and Recognition for Real-time Music Performance*. PhD diss., Carnegie Mellon University, 2013.
- [35] G.A. Ten Holta, M.J.T. Reindersa and E.A. Hendriks. *Multi-Dimensional Dynamic Time Warping for Gesture Recognition*. Thirteenth annual conference of the Advanced School for Computing and Imaging. Vol. 300. 2007.
- [36] J. Wang, A. Balasubramanian, L. Mojica de la Vega, J. R. Green, A. Samal, and B. Prabhakaran. *Word recognition from continuous articulatory movement time-series data using symbolic representations*, ACL/ISCA Interspeech Workshop on Speech and Language Processing for Assistive Technologies, Grenoble, France, 119-127 (2013).
- [37] J. Wang, A. Samal and J. R. Green. *Preliminary test of a real-time, interactive silent speech interface based on electromagnetic articulograph*, ACL/ISCA Workshop on Speech and Language Processing for Assistive Technologies, Baltimore, MD, 38-45, 2014.
- [38] J. Wang, A. Samal, J. R. Green and F. Rudzicz. *Whole-word recognition from articulatory movements for silent speech interfaces*, Proc. of Interspeech, Portland, OR, 1327-30, 2012.
- [39] L. Ye and E. J. Keogh. *Time Series Shapelets: A New Primitive for Data Mining*. KDD 2009.
- [40] S. E. Yuksel , J. N. Wilson and P. D. Gader. *Twenty years of mixture of experts*, IEEETrans. Neural Netw. Learn. Syst., vol. 23, no. 8, pp.1177 -1193 2012.
- [41] Y. Yunusova, J. R. Green and A. Mefferd. *Accuracy assessment for AG500 electromagnetic articulograph*. Journal of Speech, Language, and Hearing Research, 52, 547-555, 2009.
- [42] Q. Zhu, E. J. Keogh: *Mother Fugger: Mining Historical Manuscripts with Local Color Patches*. ICDM 2010: 699-708
- [43] Project webpage: <https://sites.google.com/site/dtwAdaptive>, While under review, files are pass protectd by DMKD2015